

DEVELOPMENT OF BENCHMARK EXAMPLES FOR DELAMINATION ONSET AND FATIGUE GROWTH PREDICTION*

Ronald Krueger

Associate Research Fellow, National Institute of Aerospace, USA

KEYWORDS

Composites, delamination, fracture mechanics, virtual crack closure technique, benchmarking

SUMMARY

An approach for assessing the delamination propagation and growth capabilities in commercial finite element codes was developed and demonstrated for the Virtual Crack Closure Technique (VCCT) implementations in ABAQUS[®]. The Double Cantilever Beam (DCB) specimen was chosen as an example. First, benchmark results to assess delamination propagation capabilities under static loading were created using models simulating specimens with different delamination lengths. For each delamination length modeled, the load and displacement at the load point were monitored. The mixed-mode strain energy release rate components were calculated along the delamination front across the width of the specimen. A failure index was calculated by correlating the results with the mixed-mode failure criterion of the graphite/epoxy material. The calculated critical loads and critical displacements for delamination onset for each delamination length modeled were used as a benchmark. The load/displacement relationship computed during automatic propagation should closely match the benchmark case. Second, starting from an initially straight front, the delamination was allowed to propagate based on the algorithms implemented in the commercial finite element software. The load-displacement relationship obtained from the propagation analysis results and the benchmark results were compared. Good agreements could be achieved by selecting the appropriate input parameters, which were determined in an iterative procedure.

*Invited keynote lecture presented at the *NAFEMS* World Congress, Boston, Massachusetts, USA, May 23-26, 2011.

DEVELOPMENT OF BENCHMARK EXAMPLES FOR DELAMINATION ONSET AND FATIGUE GROWTH PREDICTION

A benchmark case to assess the fatigue growth prediction capabilities was also created. In a first step, the number of cycles to delamination onset was calculated from the material data for mode I fatigue delamination growth onset. Then, the number of cycles during stable delamination growth was obtained incrementally from the material data for mode I fatigue delamination propagation. For the benchmark case, where the results for delamination onset and growth were combined, the delamination length was calculated for an increasing total number of load cycles. A delamination growth prediction analysis that accounts for delamination fatigue onset as well as stable growth should therefore yield results that closely resemble the benchmark curve fit. Starting from an initially straight front, the delamination was allowed to grow under cyclic loading in a finite element model. The number of cycles to delamination onset and the number of cycles during stable delamination growth for each growth increment were obtained from the analysis. Input control parameters were varied to study the effect on the computed delamination growth. The benchmarks enabled the selection of the appropriate input parameters that yielded good agreements between the results obtained from the automated analysis and the benchmark results. Overall, the results are encouraging but further assessment for mixed-mode delamination is required.

1: INTRODUCTION

The virtual crack closure technique (VCCT) (Rybicki and Kanninen, 1977; Krueger, 2004) is widely used for computing energy release rates based on results from finite element analyses and to supply the mode separation required when using a mixed-mode fracture criterion to predict delamination onset or growth. As new methods for analyzing composite delamination are incorporated in finite element codes, the need for benchmarking becomes important since each code requires specific input parameters unique to its implementation. Once the parameters have been identified, they may then be used with confidence to model delamination growth for more complex configurations.

The current paper summarizes the development of benchmark examples used to assess the automated delamination propagation and delamination growth capabilities in commercial finite element codes (Krueger, 2008, 2010; Orifici and Krueger, 2010). The creation of benchmark cases based on the Double Cantilever Beam (DCB) specimen are shown step-by-step. The creation step is independent of the software used. After creating the benchmark, the approach is demonstrated for the automated analysis in the commercial finite element code ABAQUS[®]. Starting from an initially straight front, the delamination is allowed to grow based on the algorithms implemented into the commercial finite element software. Input control parameters are varied to study the effect on the computed delamination propagation and growth. Results obtained from the automated analysis should closely match the results created manually to obtain the benchmark example.

DEVELOPMENT OF BENCHMARK EXAMPLES FOR DELAMINATION ONSET AND FATIGUE GROWTH PREDICTION

2: SPECIMEN AND MODEL DESCRIPTION

For the current numerical investigation, the Double Cantilever Beam (DCB), as shown in Figure 1, was chosen. The DCB specimen is used to determine the mode I interlaminar fracture toughness, G_{IC} . Typical two- and three-dimensional finite element models of the DCB specimen are shown in Figures 2 and 3. Along the length, all models were divided into different sections with different mesh refinement. The specimen was modeled with six elements through the specimen thickness. The plane of delamination was modeled as a discrete discontinuity in the center of the specimen. To create the discrete discontinuity, each model was created from separate meshes for the upper and lower part of the specimens with identical nodal point coordinates in the plane of delamination. Two surfaces (top and bottom surface) were created on the meshes as shown in Figure 3. Additionally, a node set was created to identify the intact (bonded nodes) region. The initial delamination front is highlighted in red. The modelling is discussed in detail in related reports (Krueger, 2008, 2010).

3: CREATING A BENCHMARK SOLUTION FOR STATIC LOADING

First, models simulating specimens with seven different delamination lengths ($30 \text{ mm} \leq a_0 \leq 40 \text{ mm}$) were analyzed. For each delamination length modeled, the reaction loads P at the location of the applied displacement were calculated and plotted versus the applied opening displacement $\delta/2$ as shown in Figure 4. The mode I strain energy release rate was calculated along the delamination front across the width of the specimen. The critical load, P_{crit} , when the failure index in the center of the specimen ($y/B=0$) reaches unity ($G_T/G_c=1$), can be calculated based on the relationship between load P and the energy release rate

$$G = \frac{P^2}{2} \cdot \frac{\partial C_P}{\partial A} \quad (1)$$

In equation (1), C_P is the compliance of the specimen and ∂A is the increase in surface area corresponding to an incremental increase in load or displacement at fracture. The critical load P_{crit} and critical displacement $\delta_{crit}/2$ were calculated for each delamination length modeled

$$\frac{G_T}{G_c} = \frac{P^2}{P_{crit}^2} \Rightarrow P_{crit} = P \sqrt{\frac{G_c}{G_T}}, \quad \delta_{crit} = \delta \sqrt{\frac{G_c}{G_T}} \quad (2)$$

and the results were included in the load/displacement plots as shown in Figure 4 (solid red circles). The results indicate that, with increasing delamination length, less load is required to extend the delamination. This means that the DCB specimen exhibits unstable delamination propagation under load control. Therefore, prescribed opening displacements $\delta/2$ were

DEVELOPMENT OF BENCHMARK EXAMPLES FOR DELAMINATION ONSET AND FATIGUE GROWTH PREDICTION

applied in the analysis instead of nodal point loads P to avoid problems with numerical stability of the analysis. It was assumed that the critical load/displacement results can be used as a benchmark. For the delamination propagation, therefore, the load/displacement results obtained from the model of a DCB specimen with an initially straight delamination of $a=30$ mm length should correspond to the critical load/displacement path (solid red line) in Figure 4.

4: RESULTS FROM AUTOMATED PROPAGATION ANALYSES

A set of example results are shown in Figure 5 where the computed resultant force (load P) at the tip of the DCB specimen is plotted versus the applied crack tip opening ($\delta/2$) for different input parameters. To overcome the convergence problems, the methods implemented in ABAQUS® were used individually to study the effects. First, global stabilization was added to the analysis. For a stabilization factor of 2×10^{-5} , the stiffness changed to almost infinity once the critical load was reached causing the load to increase sharply (plotted in red). The load increased until a point was reached where the delamination propagation started and the load gradually decreased following a saw tooth curve with local rising and declining segments. The gradual load decrease followed the same trend as the benchmark curve (in grey) but is shifted toward higher loads. For a stabilization factor of 2×10^{-6} (in green), the same saw tooth pattern was observed but the average curve was in good agreement with the benchmark result. Second, contact stabilization was added to the analysis. For all combinations of stabilization factors and release tolerances, a saw tooth pattern was observed, where the peak values were in good agreement with the benchmark result (example plotted in blue). Third, viscous regularization was added to the analysis to overcome convergence problems. Convergence could not be achieved over a wide range of viscosity coefficients when a default release tolerance value of 0.2 was used. Subsequently, the release tolerance value was increased. For all combinations of the viscosity coefficient and release tolerance, where convergence was achieved, a saw tooth pattern was obtained, where the peak values were in good agreement with the benchmark result (example plotted in black).

The examples shown highlight the importance of benchmarking to identify critical analysis input parameters. In summary, good agreement between the load-displacement relationship obtained from the propagation analysis results and the benchmark results could be achieved by selecting the appropriate input parameters. However, selecting the appropriate VCCT input parameters such as release tolerance, global or contact stabilization and viscous regularization, was not straightforward and often required an iterative procedure. The default setting for global stabilization yielded unsatisfactory results although the analysis converged. The detailed results for ABAQUS® are discussed in detail in a related report (Krueger, 2008). The results of a similar study using the

DEVELOPMENT OF BENCHMARK EXAMPLES FOR DELAMINATION ONSET AND FATIGUE GROWTH PREDICTION

same approach for the finite element codes Marc and MSC.Nastran were published recently (Orifici and Krueger, 2010).

5: CREATING A BENCHMARK SOLUTION FOR CYCLIC LOADING

For the cyclic loading of the specimen, guidance was taken from a draft standard designed to determine mode I fatigue delamination propagation. In the draft document, it is recommended to start the test at a maximum displacement, δ_{max} , which causes the energy release rate at the front, G_{Imax} , to reach initially about 80% of G_{Ic} . The maximum load, P_{max} , and maximum displacement, $\delta_{max}/2$, were calculated using the known quadratic relationship between energy release rate and applied load or displacement given in equation (2). For the current study, a critical energy release rate $G_{Ic}=0.17 \text{ kJ/m}^2$ was used and the critical values P_{crit} and δ_{crit} (grey dashed lines) were obtained from the benchmark for static delamination propagation shown in the load-displacement plot in Figure 6. The calculated maximum load, P_{max} , and calculated maximum displacement, $\delta_{max}/2$, are shown in Figure 6 (dashed red line) in relationship to the static benchmark case (solid grey circles and dashed grey line) mentioned above. During constant amplitude cyclic loading of a DCB specimen under displacement control, the applied maximum displacement, $\delta_{max}/2=0.67 \text{ mm}$, is kept constant while the load drops as the delamination length increases (solid red circles and solid red line). The energy release rate corresponding to an applied maximum displacement $\delta_{max}/2=0.67 \text{ mm}$ was calculated for different delamination lengths a using equation (2). The energy release rate decreases with increasing delamination length, a , as shown in Figure 7 (solid red circles and solid red line). Delamination growth was assumed to stop once the calculated energy release rate drops below the cutoff value, G_{th} , (green solid horizontal line). The static benchmark case (solid grey circles and dashed grey line in Figure 7), where the delamination propagates at constant G_{Ic} (solid blue line in Figure 7) was included for comparison.

The number of cycles to delamination onset, N_D , can be obtained from the delamination onset curve which is a power law fit of experimental data obtained from a DCB test using the respective standard for delamination growth onset. Details are discussed in a related report (Krueger, 2010). Solving for N_D yields

$$G = m_0 \cdot N_D^{m_1} \Rightarrow N_D = \underbrace{\left(\frac{1}{m_0} \right)^{\frac{1}{m_1}}}_{c_1} \cdot G^{\frac{1}{m_1}} \Rightarrow N_D = c_1 \cdot G^{c_2}, \quad c_2 = \frac{1}{m_1} \quad (3)$$

At the beginning of the test, the specimen is loaded initially so that the energy release rate at the front, G_{Imax} , reaches about 80% of G_{Ic} corresponding to

DEVELOPMENT OF BENCHMARK EXAMPLES FOR DELAMINATION ONSET AND FATIGUE GROWTH PREDICTION

$G_{lmax}=0.1362 \text{ kJ/m}^2$. From the delamination onset curve, the number of cycles to delamination onset is determined as, $N_D=150$.

The number of cycles during stable delamination growth, N_G , can be obtained from the fatigue delamination propagation relationship (Paris Law). The delamination growth rate (solid purple line) can be expressed as a power law function

$$\frac{da}{dN} = c \cdot G_{max}^n \quad \text{or} \quad \frac{\Delta a}{\Delta N} = c \cdot G_{max}^n \quad (4)$$

where da/dN is the increase in delamination length per cycle and G_{max} is the maximum energy release rate at the front at peak loading. The factor c and exponent n are obtained by fitting the curve to the experimental data obtained from DCB tests. A cutoff value, G_{th} , was chosen below which delamination growth was assumed to stop. Details are discussed in a related report (Krueger, 2010). Note, that this benchmarking exercise ignores branching, or fiber bridging. Hence, the Paris Law was not normalized with the static R-curve as recently suggested (Krueger, 2010).

For the current study, increments of $\Delta a=0.1 \text{ mm}$ were chosen. Starting at the initial delamination length $a_0=30.5 \text{ mm}$, the energy release rates $G_{i,max}$ were obtained for each increment, i , from the curve fit (solid red circles and solid red line) plotted in Figure 7. These energy release rate values were then used to obtain the increase in delamination length per cycle or growth rate $\Delta a/\Delta N$ from the Paris Law. The number of cycles during stable delamination growth, N_G , was calculated by summing the increments ΔN_i

$$N_G = \sum_{i=1}^k \Delta N_i = \sum_{i=1}^k \frac{1}{c} G_{i,max}^{-n} \cdot \Delta a \Rightarrow a = a_0 + \sum_{i=1}^k \Delta a = a_0 + k \cdot \Delta a \quad (5)$$

where k is the number of increments. The resulting delamination length, a , was calculated by adding the incremental lengths Δa to the initial length a_0

For the combined case of delamination onset and growth, the total life, N_T , may be expressed as $N_T = N_D + N_G$ where, N_D , is the number of cycles to delamination onset and N_G , is the number of cycles during delamination growth. For this combined case, the delamination length, a , is plotted in Figure 8 for an increasing number of load cycles N_T . For the first N_D cycles, the delamination length remains constant (horizontal red line), followed by a growth section where - over N_G cycles - the delamination length increases following the Paris Law (crosses and solid red line). Once a delamination length is reached where the energy release rate drops below the assumed cutoff value, G_{th} , (as shown in Figure 7), the delamination growth no longer follows the Paris Law (dashed grey line) and stops (horizontal solid red line). A

DEVELOPMENT OF BENCHMARK EXAMPLES FOR DELAMINATION ONSET AND FATIGUE GROWTH PREDICTION

delamination length prediction analysis that accounts for delamination fatigue onset as well as stable growth should yield results that closely resemble the plot in Figure 8. The curve fit (solid red line) can therefore be used as a benchmark.

6: RESULTS FROM AUTOMATED GROWTH ANALYSES

A set of example results are shown in Figure 9 where the delamination length, a , is plotted versus the number of cycles, N , for different input parameters and models. For all results shown, the analysis stopped when a 10,000,000 cycles limit - used as input to terminate the analysis - was reached.

First, the effect of the initial time increment used in the analysis settings was studied as shown in Figure 9. The initial time increment was varied between $i_0=0.01$ (one tenth of a single loading cycle, $t_s=0.1s$, open blue circles and solid blue line) and $i_0=0.0001$ (one thousandth of a single loading cycle, open green diamonds and solid green line). For larger initial time increments, the onset of delamination shifted towards a lower number of cycles. Reducing the initial time increments, however, significantly increased the computation time. Based on the results, it was therefore decided to use an initial time increment of $i_0=0.001$ (open red squares and solid red line) for the remainder of the study to save computation time. This step is justified by the fact that the results obtained for $i_0=0.001$ were almost identical to the values obtained from the analysis where a smaller initial time increment was used ($i_0=0.0001$). Second, the release tolerance was varied. In the current study, varying the input between 0.2 (the default value) and 0.01 did not have any effect on the computed onset and growth behavior during the analysis. It is assumed that the release tolerance only affects static delamination propagation and not growth under cyclic loading studied here. Stabilization (to overcome the convergence problems) which was required for the automated delamination propagation under static loading, was not required for automated growth analysis under cyclic loading. However input parameters to define the cyclic loading were varied and showed different affects on the computed results. Also, solution controls had to be manipulated to achieve reasonable computation times. The results from these studies are discussed in detail in a related report (Krueger, 2010).

7: CONCLUSIONS

The development of two benchmark examples for static delamination propagation and cyclic delamination growth prediction were presented and demonstrated for the commercial finite element code ABAQUS® Standard. The example was based on a finite element model of a Double Cantilever Beam (DCB) specimen, which is independent of the analysis software used and allows the assessment of the delamination propagation and growth prediction capabilities in commercial finite element codes. The development of the

DEVELOPMENT OF BENCHMARK EXAMPLES FOR DELAMINATION ONSET AND FATIGUE GROWTH PREDICTION

benchmark examples was presented step by step. Starting from an initially straight front, the delamination was then allowed to propagate or grow under cyclic loading using automated analyses.

With respect to benchmarking, the results showed the following:

- Benchmark examples for the assessment of automated delamination propagation and growth capabilities can easily be developed from a set of static analyses of models with different initial delamination lengths.
- The development of benchmark examples is independent of the software used and independent of experimental results.
- The benchmarking process can be used to identify the issues associated with the input of a particular finite element code or implementation
- Benchmarking helps identify relevant input parameters so that they may be used with confidence when modelling more complex configurations.

In general, good agreement between the results obtained from the propagation and growth analysis and the benchmark results could be achieved by selecting the appropriate input parameters. Overall, the results are promising. In a real case scenario, however, where the results are unknown, obtaining the right solution will remain challenging. Further studies are required which should include the assessment of the propagation capabilities in more complex mixed-mode specimens and on a structural level.

REFERENCES

- Rybicki E.F. and Kanninen, M.F., 1977. A Finite Element Calculation of Stress Intensity Factors by a Modified Crack Closure Integral. *Engineering Fracture Mechanics*, (9), pp. 931-938.
- Krueger, R., 2004. Virtual Crack Closure Technique: History, Approach and Applications. *Applied Mechanics Reviews*, (57), pp. 109-143.
- Krueger, R., 2008. An Approach to Assess Delamination Propagation Simulation Capabilities in Commercial Finite Element Codes, *NASA/TM-2008-215123*.
- Orifici, A.C. and Krueger, R., 2010. Assessment of Static Delamination Propagation Capabilities in Commercial Finite Element Codes Using Benchmark Analysis. *NASA/CR-2010-216709, NIA report no. 2010-03*.
- Krueger, R., 2010. Development of a Benchmark Example for Delamination Fatigue Growth Prediction. *NASA/CR-2010-216723, NIA report no. 2010-04*.

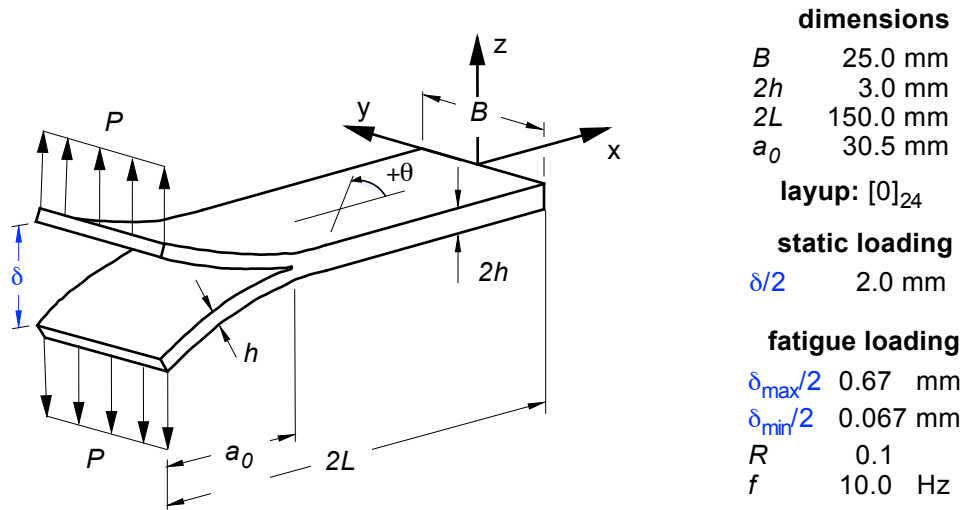


Figure 1: Double Cantilever Beam (DCB) Specimen.

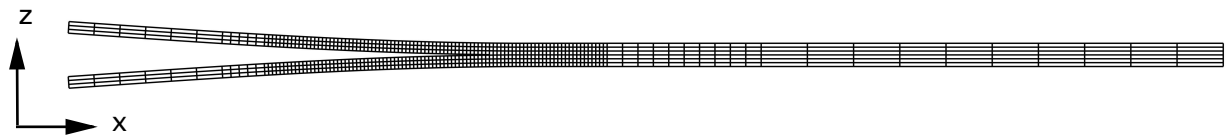


Figure 2: Deformed model of a DCB specimen (plane strain-CPE4 and plane stress-CPS4)

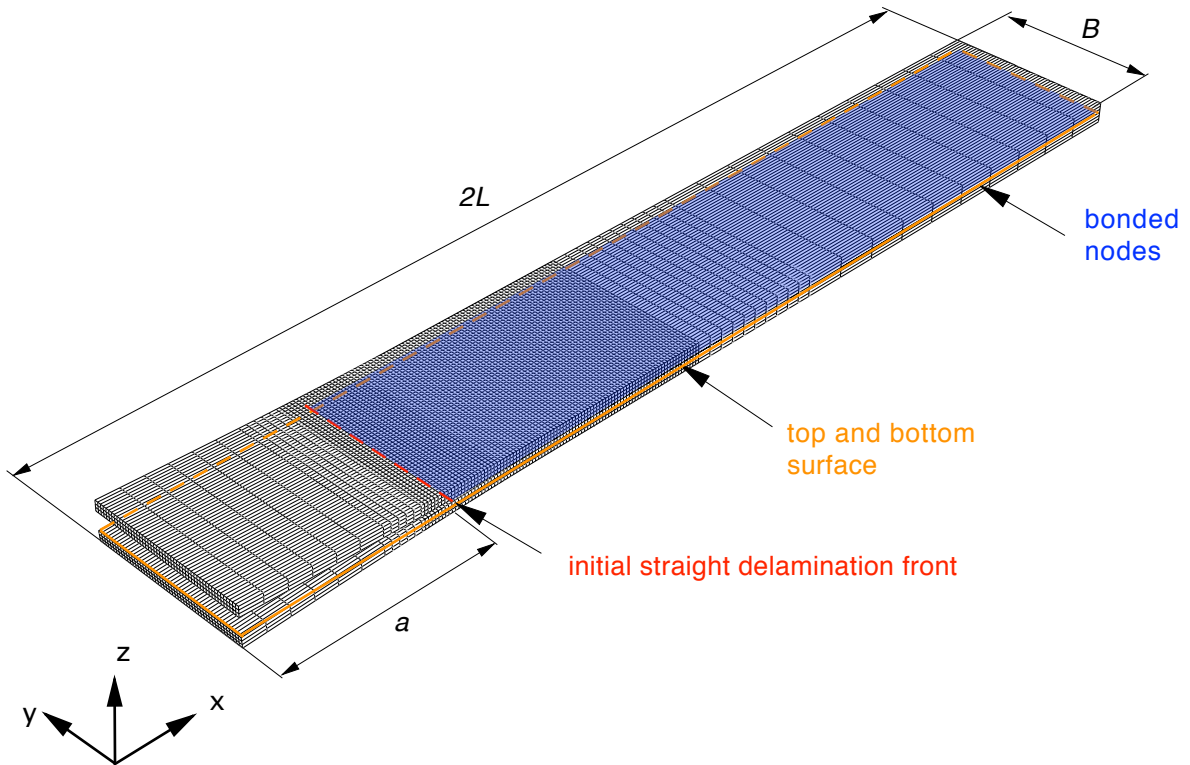


Figure 3: Full three-dimensional (solid C3D8I) finite element model of a DCB specimen.

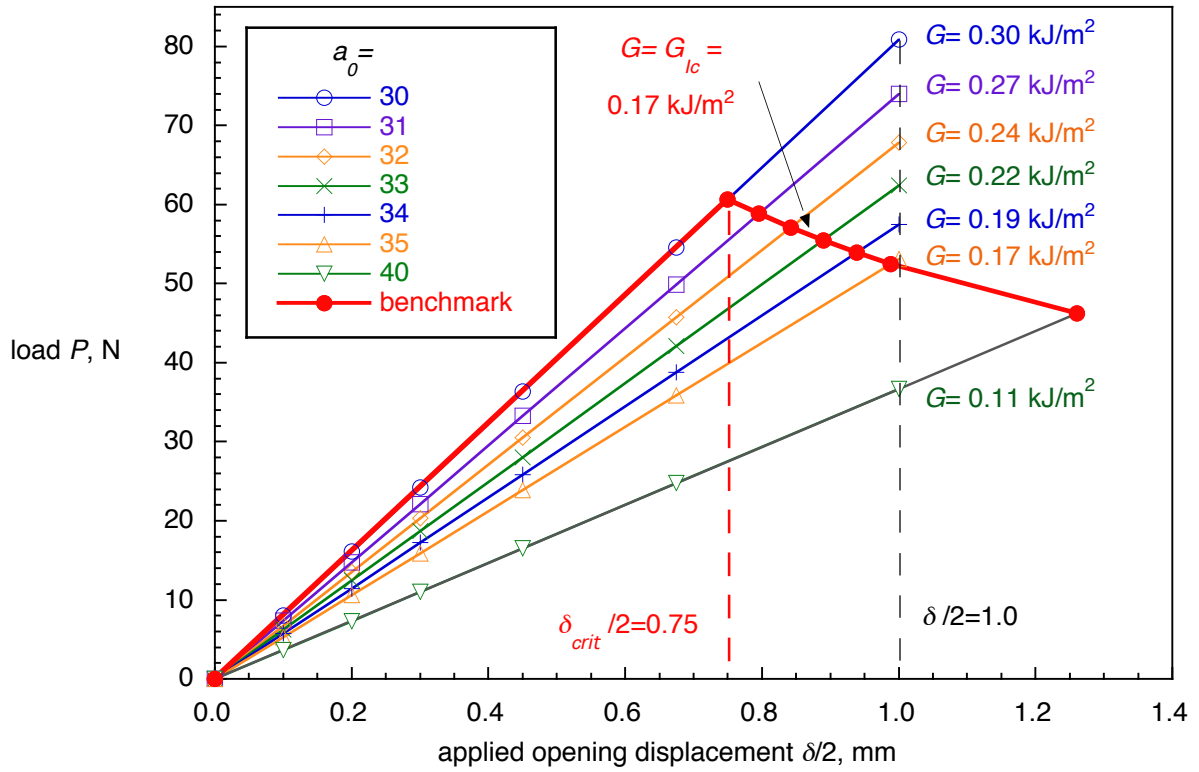


Figure 4: Calculated critical behavior and resulting benchmark case

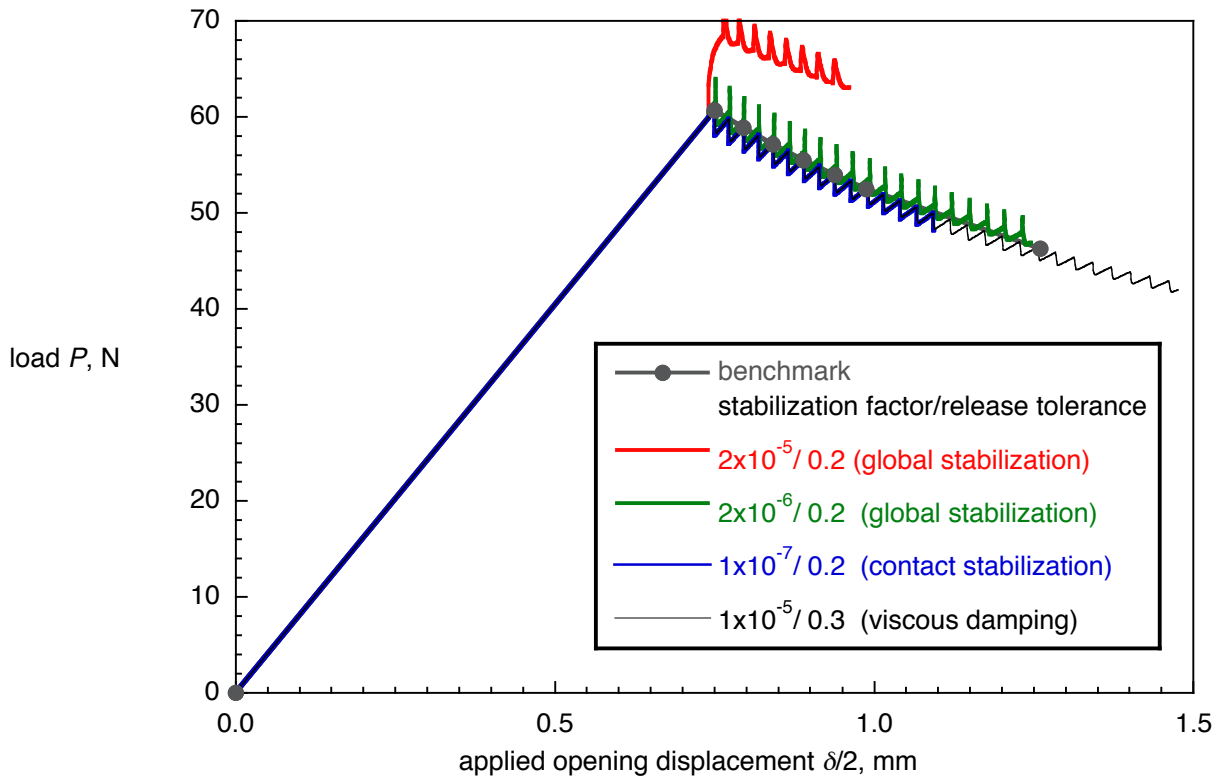


Figure 5. Computed load-displacement behavior obtained from automated analysis

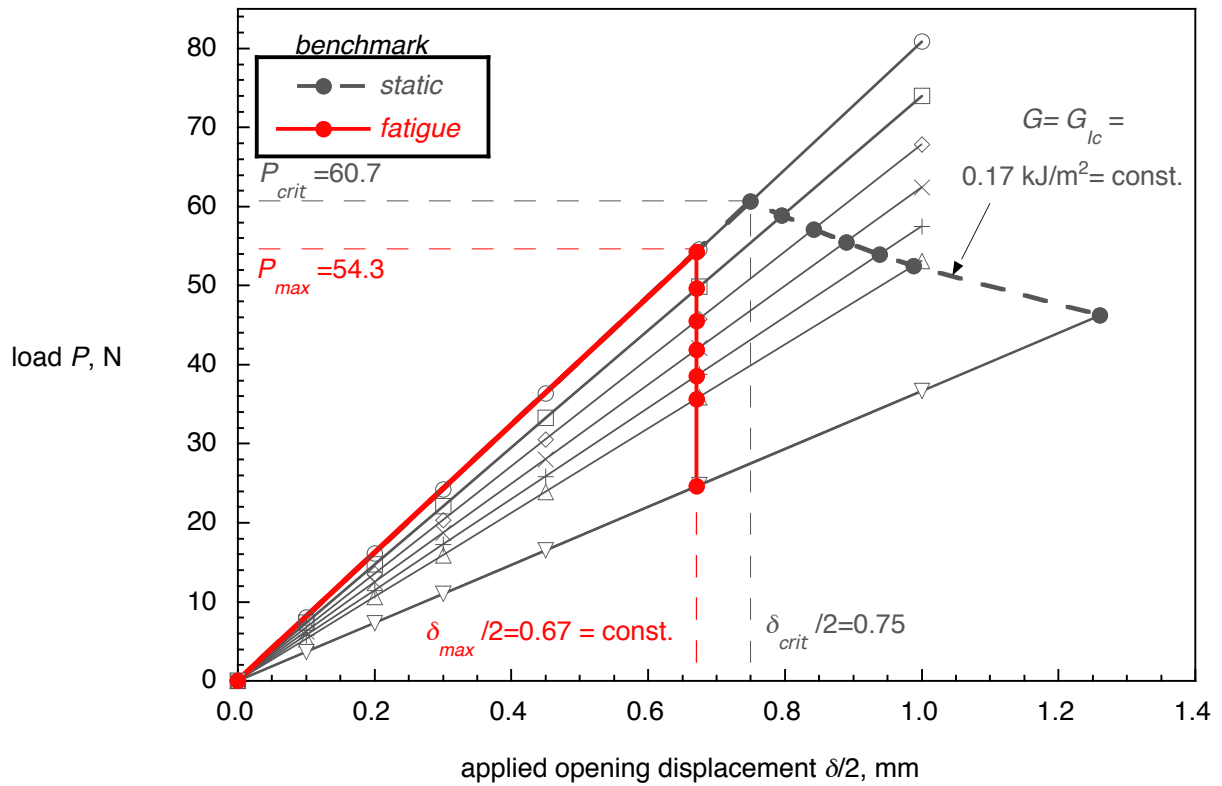


Figure 6. Critical load-displacement behavior for a DCB specimen.

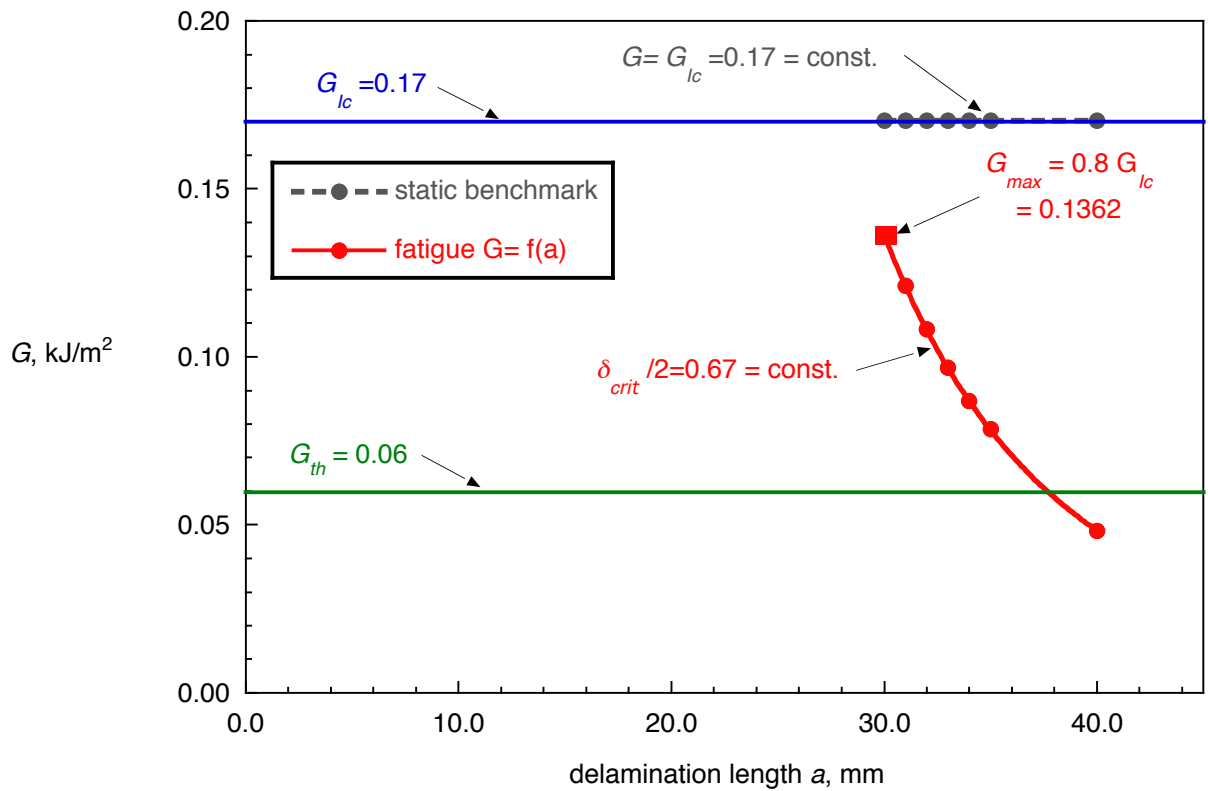


Figure 7. Energy release rate - delamination length behavior for DCB specimen.

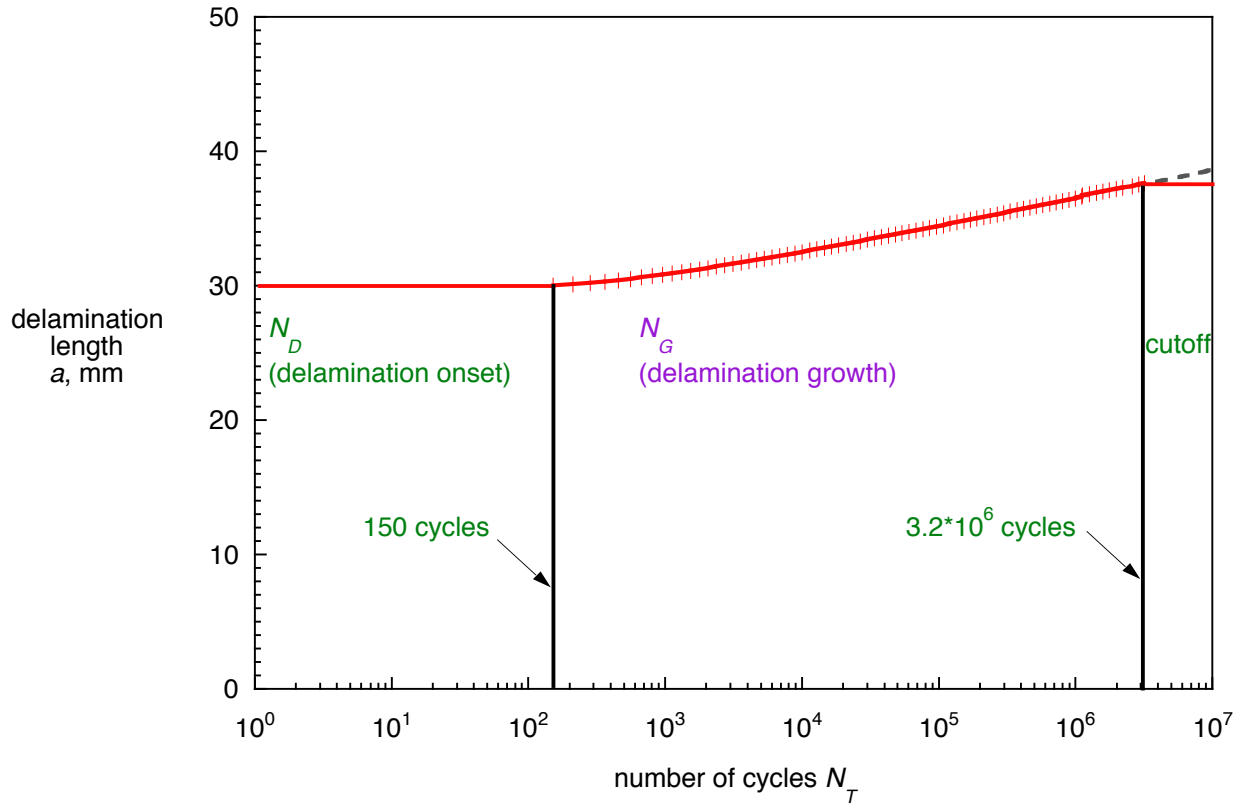


Figure 8. Delamination onset and growth behavior for DCB specimen.

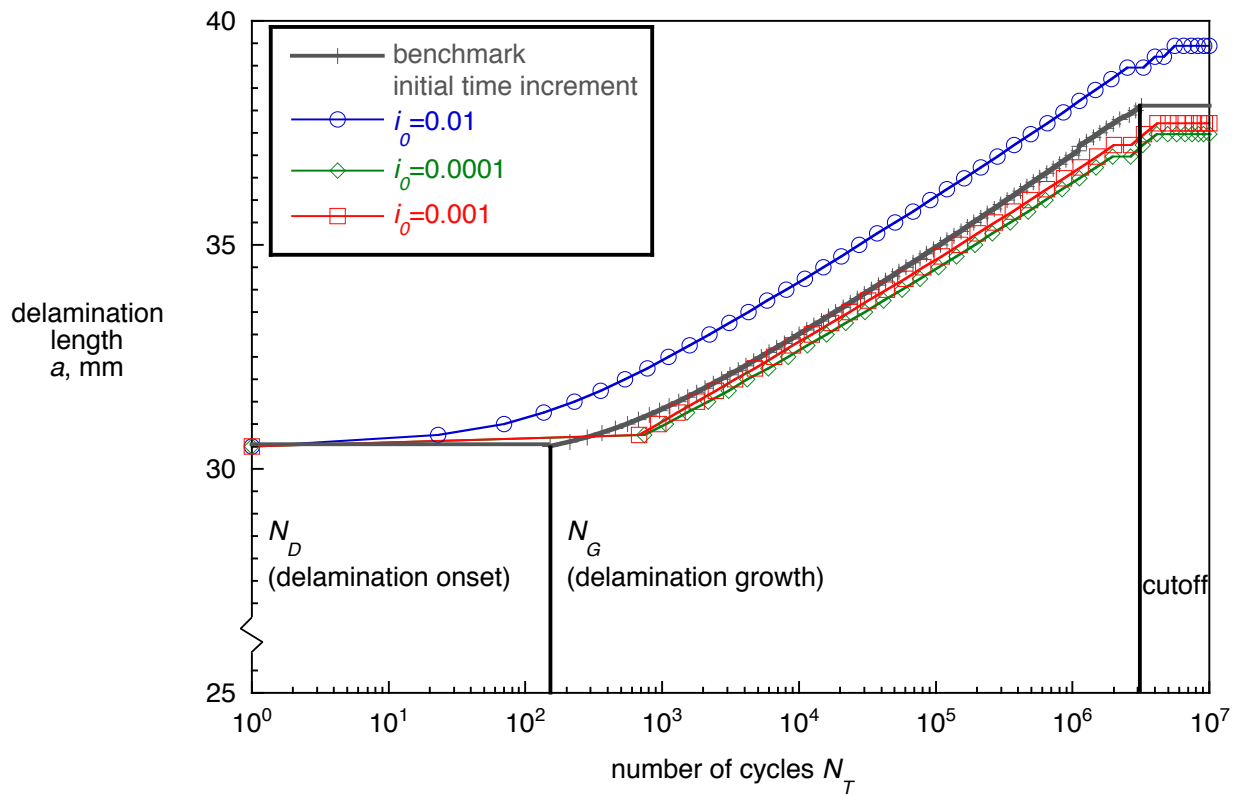


Figure 9. Computed delamination onset and growth obtained for different initial time increments.